

SAND92-0652C

Thermal Control System for SSF Sensor/Electronics¹

R. L. Akau

Thermal and Fluid Engineering Department

D. E. Lee

Engineering Design Department

Sandia National Laboratories

Albuquerque, NM 87185

ABSTRACT

A thermal control system has been designed for the SSF sensor/electronics box (SSTACK). Multi-layer insulation and heaters are used to maintain the temperatures of the critical components within their operating and survival temperature limits. Detailed and simplified SSTACK thermal models were developed and temperatures were calculated for worst-case orbital conditions. A comparison between the two models showed very good agreement. Temperature predictions were also compared to measured temperatures from a thermal-vacuum test.

INTRODUCTION

As part of the Defense Meteorological Support Program (DMSP) with Martin Marietta Astro-Space Division (MMASD), a thermal control system was designed for the SSF (Special Sensor F) sensor/electronics box (SSTACK) located on the precision mounting platform (PMP) of the DMSP satellite. The SSTACK is attached to an aluminum mounting bracket which is thermally isolated from the PMP. The top half of the SSTACK consists of an array of earth facing infrared sensors and a chopper motor, and the bottom half contains a row of electronic circuit boards. Detailed and simplified thermal models of the SSTACK were developed using the thermal analyzer SINDA [1]. The simplified thermal model was integrated into the MMASD PMP thermal model. An SSTACK TRASYS [2] geometric math model of the simplified model was also developed and incorporated into MMASD's TRASYS PMP model.

The boundary temperatures, orbital heat rates, and thermal radiation conductances from MMASD's PMP and TRASYS models for hot (95° sun angle and end-of life (EOL) optical properties) and cold (0° sun angle and beginning-of-life (BOL) optical properties)

¹This work performed at Sandia National Laboratories, supported by the U.S. Department of Energy under contract DE-AC04-76DP00789

orbits were used in Sandia Labs detailed SSTACK SINDA model. The model guided the development of the SSTACK thermal control system design which maintained the sensors, motor, and electronic board temperatures within their operational and survival temperature limits. Survival/operational heaters were required for SSTACK cold orbit thermal management. Results from the SSTACK thermal models for the different orbits will be presented and results compared to measured temperatures from a thermal-vacuum test.

DESCRIPTION OF SSF SENSOR/ELECTRONICS BOX

The SSTACK is located on the earth-facing side of the precision-mounted platform (PMP) and is attached to an aluminum bracket as illustrated in Figure 1. Figure 1 shows only the PMP and the ESM (equipment support module) sections of the DMSP satellite. The bracket is covered with multi-layer insulation (MLI) and is thermally isolated from the PMP. The PMP temperature range is $5^{\circ}\text{C} \pm 3^{\circ}\text{C}$. A schematic diagram of an earlier SSTACK design is shown in Figure 2. The SSTACK is divided into four quadrants (Q1 to Q4) with Q3 facing outward and Q1 facing inward to the spacecraft. The SSTACK has a mass of 10 kilograms (22 pounds) and produces a power of 11.5 ± 0.2 Watts as summarized in Table 1. Because of redundancy, there are A-side and B-side circuit boards for the SPS-14 and SHM-13 modules with either the A-side or B-side boards powered on. The SSTACK has an overall length and width of 24.8 cm (9.75 inches), and a height of 22.2 cm (8.79 inches). The SSTACK is constructed of thin aluminum sheets (0.10 cm (0.04 inches) average thickness) which are screwed to an inner aluminum frame structure. The SSTACK is attached to the PMP via four feet (1.8 cm by 2.0 cm) located on the bottom of the box. The top section consists of an array of eleven sensors and a chopper motor as illustrated in Figure 3. The bottom half contains an array of electronic circuit boards as shown in Figure 4 with the front covers removed. The circuit boards slide into frame guides and are plugged into a connector board. The front-end of the board frames, except for the two power supply module frames (SPS-14A and SPS-14B), are screwed to the inner frame structure. The front-ends of the power supply frames are attached to the box front cover which enhances heat conduction from the power supplies to the front cover. The operating and survival (power off) component temperature limits are given in Table 2.

Kapton insulated resistive strip heaters (4 Watts each and two per side) are located on the inner wall surfaces (see Figure 4). A thermal control electronics (TCE) device, provided by MMASD, is used to turn the heaters on and off at a temperature set-point of $-10 \pm 0.2^{\circ}\text{C}$. The TCE temperature sensor is located near the chopper motor (see Figure 3). Each of the eleven sensors have apertures located on the earth-facing top cover. The aperture plate is shown in Figure 5.

DESCRIPTION OF SSTACK THERMAL MODELS AND ORBIT RESULTS

The DMSP operates in a 450 NM orbit having a 100 minute orbit period. For the hot orbit, the DMSP satellite encounters an eclipse (earth's shadow) during thirty-percent of the orbit and the SSTACK receives direct solar flux immediately before and after eclipse. However, during the cold orbit, the SSTACK is shaded and does not receive any direct solar flux. MMASD required each sensor contractor to provide simplified SINDA and TRASYS models to be integrated into the MMASD PMP thermal and TRASYS models. The nodes for the reduced model are shown in Figure 6 and in Figure 7 for the detailed model which consisted of 24 and 48 diffusion nodes, respectively. The detailed model was first constructed and the simplified model was developed by maintaining the critical components (motor, sensors, and power supplies). The simplified nodes were formed by combining nodal points and calculating equivalent thermal conductances from the detailed model.

Figure 8 illustrates the MLI design and the thermal radiator surfaces. The SSTACK thermal radiator surfaces include the nadir-facing sensor aperture plate and the bottom half of Q3 which are coated with S-13 GLO white paint. The other surfaces are covered with MLI (8 layers of 0.5 mil thick double-sided aluminized Kapton, 1 mil thick black Kapton outer layer, and 0.5 mil thick Kapton inner layer).

The environmental heat fluxes (direct and reflected solar, and earthshine), boundary temperatures, and thermal radiation conductances for the hot and cold orbits were obtained from MMASD's PMP thermal and TRASYS models. The heat fluxes and boundary temperatures were input into the SSTACK thermal models. The SSTACK temperatures were calculated using the thermal analyzer SINDA until quasi steady-state conditions were obtained (approximately 18 orbits). The thermal parameters used in MMASD's PMP TRASYS model for the cold and hot orbits are shown in Table 3.

Temperature predictions and a comparison between the simplified and detailed thermal models during hot operational conditions (11.7 Watts) are given in Table 4. The temperature uncertainty for model predictions, $\pm 11^{\circ}\text{C}$, according to MIL-1540B [3] was not included in Table 4. Adding the uncertainty, the electronics modules, motor, and sensor temperatures are a few degrees above their desired maximum operating temperatures and are higher than their minimum operating temperatures. A one-Watt operational heater was needed for the morning orbit to keep the motor temperature from going below -10.2°C . A comparison between the simplified and detailed models indicate temperatures that are within $\pm 5^{\circ}\text{C}$. Results for the cold orbit (11.3 Watts) and survival conditions (power off) are shown in Table 5 where temperatures for the simplified and detailed thermal models compare to within $\pm 2^{\circ}\text{C}$. Approximately 12 Watts of survival heater power was needed to maintain the motor temperature from going below -10.2°C . However, Table 5 shows a motor temperature of -11.0°C . This was attributed to thermal lag from the

motor location to the heaters. Adding -11°C to the critical component temperatures in Table 5, indicate temperature limits well above minimum survival temperatures.

THERMAL-VACUUM TEST SET-UP

SSTACK thermal-vacuum tests were recently conducted in a 42 inch diameter by 42 inch high chamber. Thermal balance tests were performed to verify the SSTACK thermal model. The SSTACK was screwed to a block of fiberglass G-10 material to thermally isolate the SSTACK from the chamber baseplate. An MLI test blanket was built and consisted of ten layers of double-sided aluminized Kapton and an outer layer of double-sided aluminized Mylar. The outer surface of the aluminized Mylar was painted with Chemglaze Z-306 black paint. The sensor aperture plate and the bottom of Q3 were painted with S13-GLO white paint. Also included in the chamber was a power distribution box (PSTACK) that accompanies the SSTACK. The PSTACK is located in the ESM section of the DMSP satellite (see Figure 1) and was also bolted to the baseplate. The PSTACK was covered with a separate MLI blanket to minimize thermal radiation interaction with the SSTACK. The baseplate and inner wall of the chamber were controlled to preset temperatures with the chamber pressure maintained at 10^{-6} torr.

The SSTACK has 14 internal AD-590 temperature monitors on each of the sensors, the motor, and the power supplies. The AD-590's, shown in Figures 3 and 4, have an accuracy of $\pm 2^{\circ}\text{C}$, and an output voltage which corresponds to a calibrated temperature. In addition to the internal temperature monitors, copper constantan (Type-T) thermocouples were attached to the external surfaces of the SSTACK using Kapton tape illustrated in Figures 9 to 11. Thermocouples were also located on the inner wall of the chamber (shroud) and baseplate, and on the PSTACK. The thermocouples were calibrated to be $\pm 3^{\circ}\text{C}$. The thermal balance tests were conducted at three different shroud and baseplate temperature levels to simulate SSTACK hot-operational (10°C and 20°C) and cold-operational (-100°C and 20°C) conditions. A mid-point operational (-40°C and 20°C) condition was also performed as a third data point for the SSTACK thermal model. The temperature boundaries were held constant for 15 hours at each condition at which time the SSTACK temperatures changed by no more than 2°C per hour. The A-side was powered on (11.7 Watts) throughout the tests.

The boundary temperatures were determined by a thermal-vacuum thermal model which incorporated the SSTACK, PSTACK, baseplate, and shroud. A TRASYS model was developed for the SSTACK and PSTACK in the vacuum chamber in order to obtain the thermal radiation conductances for the experimental setup. Shroud and baseplate temperatures boundaries were put into the SINDA thermal model and steady-state temperatures were calculated for the three thermal balance tests. Thermal model calculations were done on a Sun Workstation.

COMPARISON OF SSTACK PREDICTED AND MEASURED RESULTS

Preliminary comparisons between the predicted and measured steady-state temperatures are given in Tables 6 to 8 for the hot-operational, cold-operational, and mid-operational tests. The model was first compared to the hot and cold cases with an SSTACK power of 11.7 Watts as shown in Tables 6 and 7. The effective emittance (ϵ^*) of the MLI was 0.02. For the hot case, Table 6, a comparison of the measured and predicted temperatures for the critical components (motor, sensors, and power supply) were within 3°C. For the cold test, Table 7, the component temperatures also compared well, but the measured cover temperatures for Q2 and Q4 (TC5 and TC15) were over 10°C lower than the calculated values even though the measured outer temperatures of the MLI surfaces for Q2 and Q4 (TC9 and TC19) were within 5°C of the calculated values. These discrepancies could be attributed to heat leaks through MLI blanket openings, and thermocouples detaching from the surface. Analysis is continuing to determine these large temperature differences.

SUMMARY AND CONCLUSIONS

A thermal control system was designed for the SSTACK located on the PMP section of the DMSP satellite. The aperture plate and the bottom of Q3 were painted with S13-GLO white paint and the remaining surfaces, except for the bottom plate, covered with MLI. A one-Watt operational heater was needed for the cold orbit and a 12-Watt survival heater for the cold orbit powered off condition. Detailed and simplified SINDA thermal models were developed for the SSTACK with the simplified model integrated into MMASD's PMP thermal model. There was very good agreement between the reduced and detailed thermal models for cold and hot orbital conditions. The model calculations were also compared to measured results from a recent thermal-vacuum test. Preliminary results indicated good agreement between measured and predicted results for the critical components (motor, sensors, and power supply).

REFERENCES

1. User's Manual for the Aerospace Version of J. Gaski's SINDA 1987/ANSI Code.
2. User's Manual Thermal Radiation Analysis System, TRASYS II ANSI Version 1.0, Martin Marietta, February 1987.
3. MIL-1540B (USAF), Military Standard Test Requirements for Space Vehicles, October 10, 1982, Department of the Air Force, Washington, D. C. 20301.

Table 1. Nominal Power Distribution for SSTACK.

Component	Power (Watts)	
	A-Side On	B-Side On
Bottom Section		
BMD-10	0.62	0.62
SPS-14A	2.15	0.00
SPS-14B	0.00	2.15
SFR-10	0.01	0.01
PAT-10	0.01	0.01
PAA-10	0.91	0.90
PAA-10	0.91	0.91
PAA-10	0.91	0.91
ARM-10	0.50	0.50
SAA-11	0.53	0.53
SAA-11	1.04	1.04
SAT-10	0.20	0.20
SHM-13A	0.33	0.00
SHM-13B	0.00	0.33
CAS-12	0.48	0.48
CAL-27	0.00	0.00
Top Section		
Motor	0.66	0.66
Pyro Sensors	1.14	1.14
Silicon Sensors	0.74	0.74
Radiometer (2)	0.35	0.35
Total	11.50	11.50

Table 2. SSTACK Component Temperature Limits.

Component	Temperature (°C)	
	Operational	Survival
Sensors	-30 to 35	-40 to 55
Motor	-23 to 35	-40 to 60
Electronics	-40 to 50	-40 to 70

Table 3. Thermal Parameters for Cold (BOL) and Hot (EOL) Orbits.

Parameter	Cold	Hot
Solar Flux (W/cm ²)	0.132	0.142
Earth Infrared (W/cm ²)	0.021	0.026
Earth Albedo	0.275	0.375
S13-GLO White Paint	α_s 0.20	ϵ_{IR} 0.42
Black Kapton 1 mil	0.87	0.87
MLI effective ϵ^*	0.05	0.02
PMP Temp. (°C)	2	8

Table 4. SSTACK Operational Orbit Temperatures.

Node No.	Simplified Model Temperature (°C)				Node No.	Detailed Model Temperature (°C)			
	Hot Orbit 11.7 Watts		Cold Orbit 11.3 Watts			Hot Orbit 11.7 Watts		Cold Orbit 11.3 Watts	
	Min.	Max.	Min.	Max.		Min.	Max.	Min.	Max.
Electronics Modules									
8012	31.9	34.9	-1.6	-0.6	1001	29.6	33.2	-5.2	-2.6
8013	27.9	36.1	-5.8	-4.7	1002	27.4	36.2	-6.5	-4.2
8014	18.4	29.2	-13.6	-12.3	1003	19.7	29.4	-14.1	-11.6
8015	26.2	30.0	-7.2	-5.5	1004,1005	28.1	30.7	-7.5	-5.5
8016	37.8	39.6	3.7	4.6	1006,1007 1008	36.6	38.7	1.2	3.2
8017	34.4	36.2	-0.1	0.8	1009	33.0	35.1	-2.8	-0.7
8018	34.4	36.2	0.3	0.8	1010	33.4	35.5	-2.4	-0.3
8029	36.8	38.1	2.9	3.3	1011-1016	33.2	34.9	-1.7	0.1
Chopper Motor									
8008	24.8	26.3	-10.2	-8.8	1017	26.6	27.8	-10.2	-8.4
Sensors									
8009	23.6	25.9	-11.2	-10.1	1018-1020	24.0	27.4	-11.8	-8.4
8010	23.0	25.8	-11.1	-8.7	1021,1022 1027,1028	25.7	27.3	-11.4	-8.4
8011	22.8	25.9	-11.2	-8.9	1023-1026	24.1	27.2	-11.4	-8.6
External Covers									
8001	16.1	32.2	-14.2	-12.6	8001	17.3	32.4	-14.6	-11.2
8002	23.0	27.8	-10.1	-6.7	8002	22.9	27.9	-11.6	-5.9
8003	23.7	28.1	-9.6	-7.3	8003	23.5	28.2	-10.9	-6.5
8004	22.9	27.8	-10.1	-6.7	8004	22.9	28.0	-11.6	-5.9
8005	17.8	25.1	-13.3	-8.0	8018	19.3	26.2	-13.5	-8.8
8006	25.6	29.3	-7.8	-6.4	8019	25.3	28.9	-9.5	-6.6
8007	27.1	30.4	-6.8	-4.9	8020	24.1	28.8	-10.5	-5.8
8021	18.4	25.4	-13.3	-9.1	8006,8010 8014	20.2	26.7	-13.2	8.3
8022	20.3	25.6	-12.2	-4.9	8007,8011 8015	21.5	26.8	-12.7	-5.9
8023	20.4	25.7	-12.1	-8.2	8008,8012 8016	21.6	26.9	-12.4	-7.6
8024	20.3	25.6	-12.2	-4.9	8009,8013 8017	21.5	26.8	-12.5	-5.8
Note: ±11°C uncertainty not included.									

Table 5. SSTACK Cold Orbit Temperatures, Power Off.

Simplified Model			Detailed Model		
Node	Temperature (°C)		Node	Temperature (°C)	
	Min.	Max.		Min.	Max.
Electronics Modules					
8012	-14.1	-13.1	1001	-15.3	-12.2
8013	-18.8	-17.7	1002	-20.1	-17.6
8014	-19.1	-17.7	1003	-20.4	-17.6
8015	-14.2	-12.3	1004,1005	-14.8	-13.0
8016	-13.6	-12.8	1006,1007 1008	-14.3	-12.0
8017	-13.5	-12.8	1009	-14.3	-12.0
8018	-13.5	-12.8	1010	-14.3	-12.1
8029	-13.4	-12.9	1011-1016	-14.1	-12.6
Chopper Motor					
8008	-10.7	-9.7	1017	-11.0	-9.4
Sensors					
8009	-12.0	-10.9	1018-1020	-12.7	-8.7
8010	-11.4	-8.3	1021,1022 1027,1028	-12.2	-8.3
8011	-11.4	-8.7	1023-1026	-12.1	-8.5
External Covers					
8001	-19.9	-17.6	8001	-21.5	-17.7
8002	-14.9	-10.5	8002	-16.5	-9.3
8003	-14.4	-11.1	8003	-15.9	-10.7
8004	-14.9	-10.5	8004	-16.7	-9.5
8005	-15.4	-8.9	8018	-15.6	-8.8
8006	-14.5	-12.7	8019	-15.8	-12.3
8007	-14.2	-11.7	8020	-16.4	-10.1
8021	-15.8	-10.6	8006,8010 8014	-17.0	-11.1
8022	-13.9	-5.8	8007,8011 8015	-15.6	-7.0
8023	-14.3	-9.2	8008,8012 8016	-15.3	-9.3
8024	-13.9	-6.1	8009,8013 8017	-15.6	-7.0
Note: $\pm 11^{\circ}\text{C}$ uncertainty not included.					

Table 6. Comparison of Measured and Calculated Temperatures, Hot-Operational.

Thermocouple		AD-590		Model	
TC No.	Temp. (°C)	AD-590	Temp. (°C)	Model Node	Temp. (°C)
Q1					
1	33.3	Box 1	37.0	8003	35.7
2	30.5	Box 2	37.0	8023	32.9
3	29.4			8023	32.9
4 (MLI)	18.1			8027	15.3
Q4					
5	28.4			8004	34.5
6	32.0			8024	32.7
7	29.6			8024	32.7
8	28.9			8024	32.7
9 (MLI)	17.7			8028	14.1
Q3					
10	36.1			8001	33.6
11				8001	33.6
12	29.1			8021	32.3
13	30.0			8021	32.3
14 (MLI)	18.4			8025	14.0
Q2					
15	26.5			8002	34.6
16	31.2			8022	32.7
17	34.5			8022	32.7
18	29.4			8022	32.7
19 (MLI)	16.7			8026	14.7
Aperture Plate					
21	33.6			8005	31.6
Motor					
			36.0	8008	34.5
Power Supply					
			47.0	8013	50.0
Sensors					
			37.0	8009-8011	34.0

Table 7. Comparison of Measured and Calculated Temperatures, Cold-Operational.

Thermocouple		AD-590		Model	
TC No.	Temp. (°C)	AD-590	Temp. (°C)	Model Node	Temp. (°C)
Q1					
1	-24.5	Box 1	-25.0	8003	-30.6
2	-28.4	Box 2	-25.0	8023	-33.4
3	-33.1			8023	-33.4
4 (MLI)	-63.6			8027	-75.6
Q4					
5	-42.1			8004	-31.8
6	-34.1			8024	-33.7
7	-39.5			8024	-33.7
8	-37.0			8024	-33.7
9 (MLI)	-83.4			8028	-81.4
Q3					
10	-25.3			8001	-32.6
11				8001	-34.1
12	-45.0			8021	-34.1
13	-45.3			8021	-34.1
14 (MLI)	-81.6			8025	-82.1
Q2					
15	-46.3			8002	-31.7
16	-39.5			8022	-33.7
17	-32.7			8022	-33.7
18	-42.9			8022	-33.7
19 (MLI)	-75.4			8026	-79.5
Aperture Plate					
21	-30.7			8005	-34.8
Motor					
			-28.0	8008	-31.8
Power Supply					
			-13.0	8013	-14.6
Sensors					
			-28.0	8009-8011	-33.0

Table 8. Comparison of Measured and Calculated Temperatures, Mid-Operational.

Thermocouple		AD-590		Model	
TC No.	Temp. (°C)	AD-590	Temp. (°C)	Model Node	Temp. (°C)
Q1					
1	3.7	Box 1	5.0	8003	-0.1
2	1.6	Box 2	5.0	8023	-2.9
3	-2.9			8023	-2.9
4 (MLI)	-20.5			8027	-29.4
Q4					
5	-5.8			8004	-1.3
6	-2.1			8024	-3.6
7	-6.5			8024	-3.6
8	-3.1			8024	-3.6
9 (MLI)	-27.1			8028	-32.3
Q3					
10	5.1			8001	-2.1
11				8001	-3.6
12	-8.3			8021	-3.6
13	-5.5			8021	-3.6
14 (MLI)	-28.9			8025	-32.3
Q2					
15	-10.1			8002	-1.3
16	-4.4			8022	-3.1
17	1.1			8022	-3.1
18	-8.0			8022	-3.1
19 (MLI)	-30.4			8026	-31.0
Aperture Plate					
21	0.1			8005	-4.3
Motor					
			3.0	8008	-1.3
Power Supply					
			16.0	8013	15.0
Sensors					
			4.5	8009-8011	-2.0

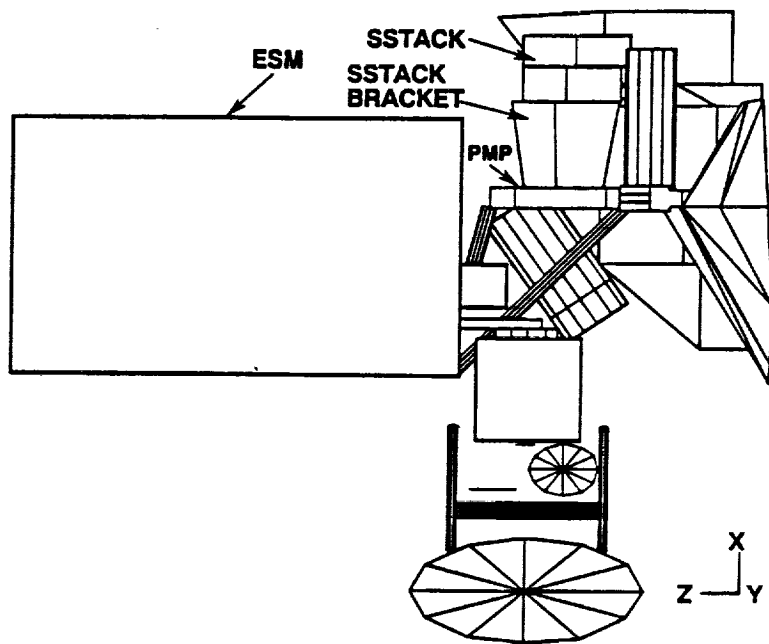


Figure 1. SSTACK location on PMP.

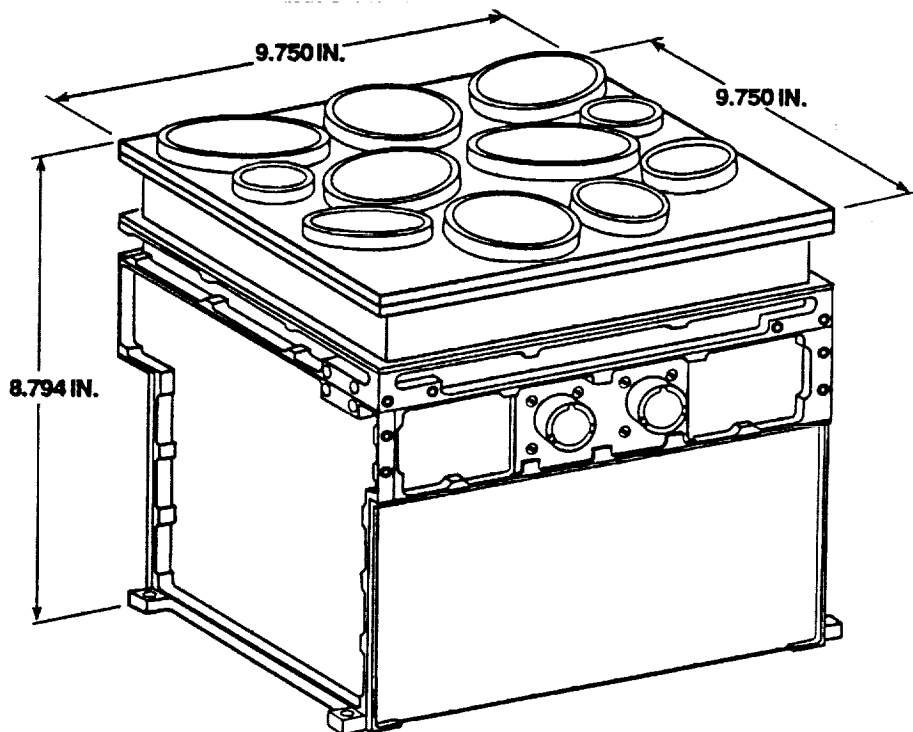


Figure 2. Schematic diagram of SSTACK.

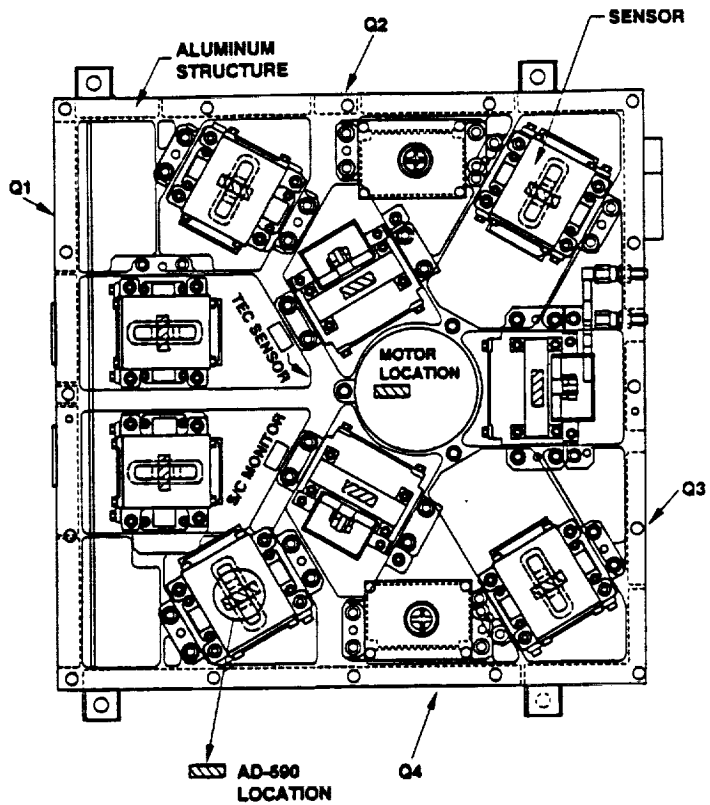


Figure 3. Top view of SSTACK showing motor and sensors.

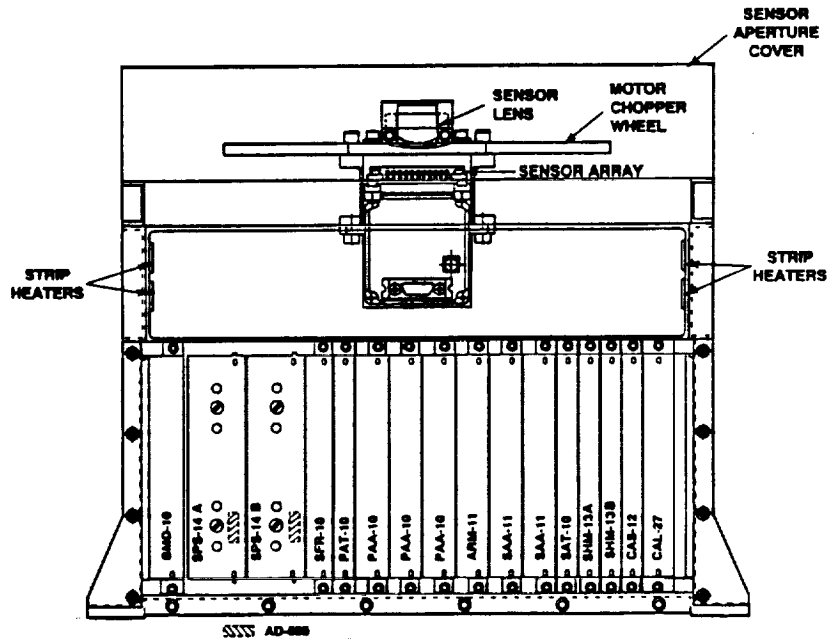


Figure 4. Front-view of SSTACK with front cover removed.

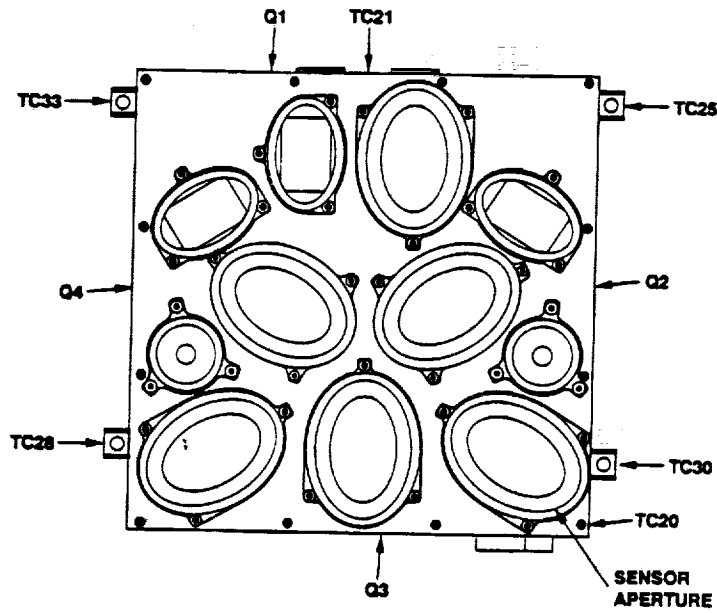


Figure 5. SSTACK aperture plate.

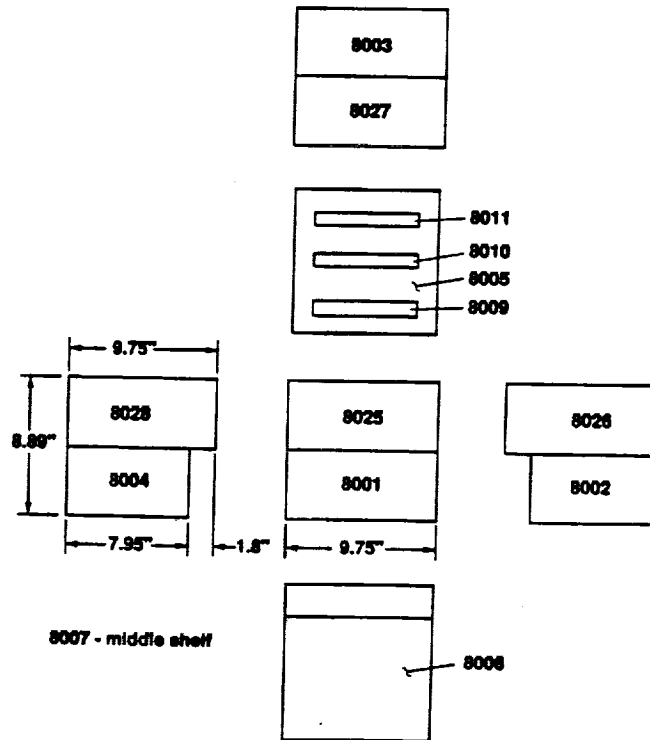


Figure 6. Reduced SINDA thermal model nodes.

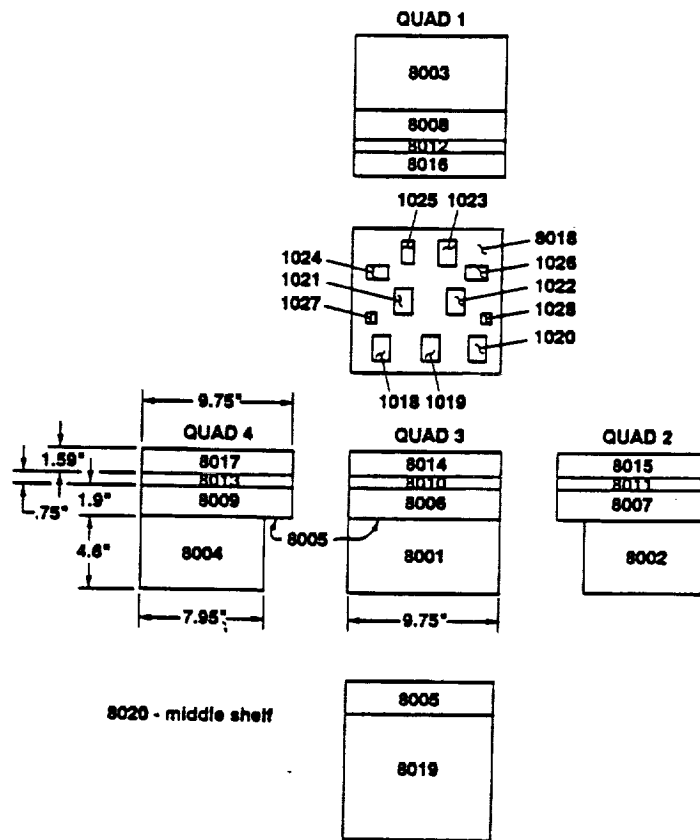


Figure 7. Detailed SINDA thermal model nodes.

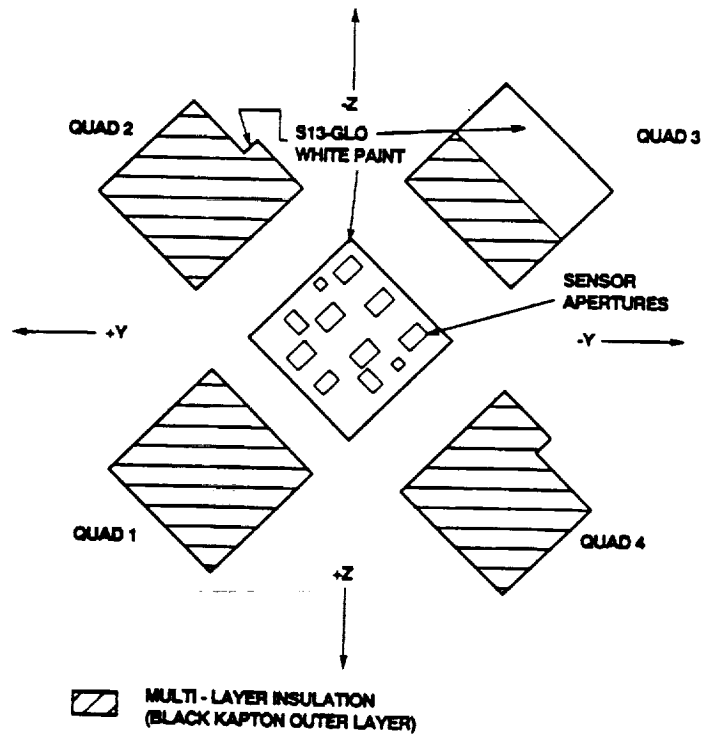


Figure 8. MLI thermal blanket design.

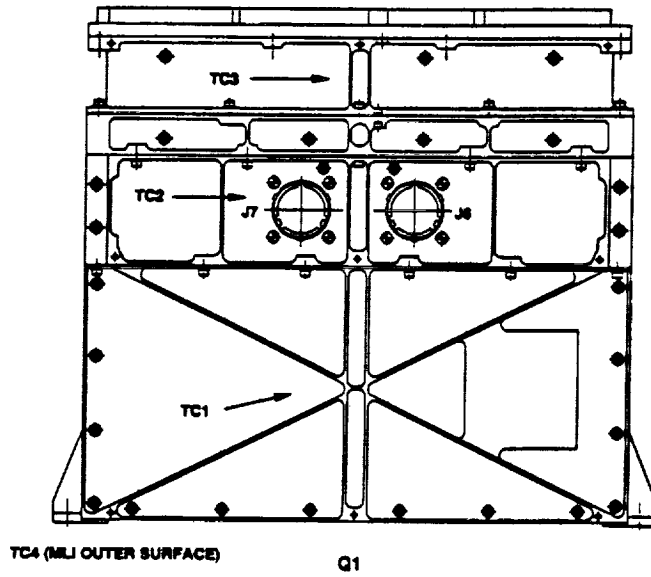


Figure 9. Thermocouples locations on Q1.

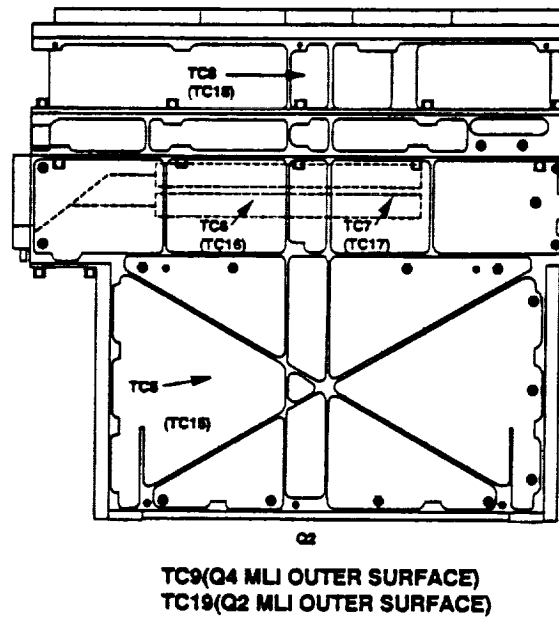
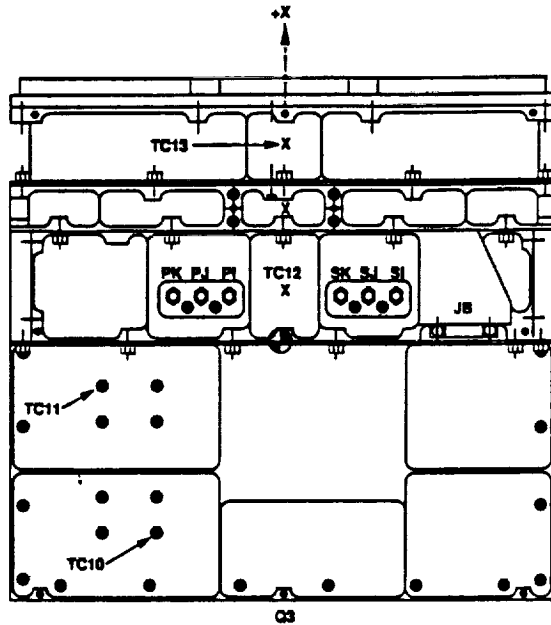


Figure 10. Thermocouples locations on Q2 (paranthesis) and Q4.



TC14 (MLI Outer Surface)

Figure 11. Thermocouples locations on Q3.

THE UNIVERSITY OF CHICAGO
DIVISION OF THE PHYSICAL SCIENCES
DEPARTMENT OF CHEMISTRY
5708 S. UNIVERSITY AVENUE
CHICAGO, ILLINOIS 60637

RECEIVED
MAY 15 1964

**Session
Two**

Refrigeration/Power Systems

PRECEDING PAGE BLANK NOT FILMED

